Selective adsorption of Pb(II) ion on amine-rich functionalized rice husk magnetic nanoparticle biocomposites in aqueous solution

by Doni Wicakso

Submission date: 02-Mar-2021 04:40PM (UTC+0700)
Submission ID: 1522162987
File name: ctionalized_rice_husk_magnetic_nanoparticle_biocomposites_in.pdf (2.66M)
Word count: 6483
Character count: 33839

Journal of Environmental Chemical Engineering 8 (2020) 104339

Contents lists available at ScienceDirect

Journal of Environmental Chemical Engineering

journal homepage: www.elsevier.com/locate/jece

Selective adsorption of Pb(II) ion on amine-rich functionalized rice husk magnetic nanoparticle biocomposites in aqueous solution

Iryanti Fatyasari Nata*, Doni Rahmat Wicakso, Agus Mirwan, Chairul Irawan, Divany Ramadhani, Ursulla

Chemical Engineering Department, Faculty of Engineering, Lambung Mangkurat University, Jl. A. Yani Km. 35.5, Banjarbaru, South Kalimantan 70714, Indonesia

ARTICLE INFO

Editor: G.L. Dotto

Keywords:
Adsorption
Pb(II) ion
Magnetic nanoparticle
Rice husk
Solvothermal

ABSTRACT

Amine group on rice husk magnetic nanoparticle bicomposites (RHB-MH) was synthesized by one-step solvothermal method. The new finding of biocomposites is utilization of rice husk cellulose as a support which produced high amine content on surface of magnetic nanoparticle (MNPs). The rice husk cellulose (RH-D), iron (III) chloride hexahydrate, Na-acetate anhydrate were mixed in ethylene glycol, then kept at ± 200 °C for 6 h. Amine modified MNPs was constructed by addition of 1,6-hexanediamine in mixture before the reaction. The MNPs was growth on surface of RH-D then formed biocomposites. The Fe content about 93.11 % and the magnetic nanoparticle structure was proved by specific peaks at 36°, 43°, 63° for magnetite. The magnetic saturation value of biocomposites about 16.4 emu/g. The thermal stability of biocomposites showed up to 200 oC with less than 10 % of mass degradation. Higher amine content of 12.3 mmol/g on biocomposites was achieved after addition of 7 mL of 1,6-hexanediamine (RBH-MH2). Amine functional group on biocomposites exhibited the resonance bands at 1645 cm^{-1} and 1050 cm^{-1}. The adsorption of Pb(II) ion on RBH-MH2 follows pseudo 1 st order kinetic and well-fitted by Langmuir adsorption isotherm model which have maximum capacity of 680.19 mg/g at room temperature and pHe ~ 5. The RBH-MH2 have significant effect to capture Pb(II) ion due to electrostatic interaction and showed 3.6-fold higher adsorption capacity than rice husk biocomposites without modification. The amine-rich on biocomposites does not only provide an easy retrievable from aqueous solution but also potential candidate for effective green adsorbent.

1. Introduction

Recently, issue of environmental is a serious topic due to big effects to the environment and human. The contamination of water due to heavy metal and organic compound as well as dye has become a great environmental concern worldwide. Generally, heavy metal ions possess high toxicities and easily accumulated on organisms through the food chain mechanism [1]. One of dangerous metal ion is lead, when severe lead poisoning causes neonatal mortality and most serious effects is to break central nervous system [2]. Lead also can damage reproductive system such as kidney, liver, basic and brain functions [3]. Recent developments in adsorption technique of heavy metal ion and dyes in aqueous solution lead to a renewed interest in surface modification of adsorbent. It was modifying by surface functionalization with specific functional groups on polymeric materials [4–9]. There are several techniques water treatment technologies to remove metal ion in aqueous solution including chemical precipitation, photo catalytic purification, microwave catalysis, precipitation, ion exchange and adsorption [10–15]. Adsorption technique is simple, effective, and has high binding capacities for manganese, iron, cadmium, and lead ion adsorption [7,16–18].

Based on economical and environmental points of view, utilization of low cost agricultural by-products is main concern on this research. Conventionally, to eliminate the rice husk (RH) as waste only by burning or covering land that can cause air pollution due to increasing of CO gas [19,20]. Beside, RH has potential application as adsorbent by functional groups on surface such as amidogen and carboxyl [21]. However, the application of RH as adsorbent could be effective by modified surface using chemicals such as mineral and organic acids like tartaric acid, sodium hydroxide, oxidizing agent, etc. via increasing the number of functional groups. RH contains of 50 % of cellulose which have light weight and better mechanical properties [22,23]. So that, RH is a potential natural fiber source as raw material to mix with MNPs for composite material. MNPs which have unique properties have been used in research such as magnetic storage [24], immunoassay [25] and photocatalyzing reaction [26,27]. The synthesis of MNPs by

* Corresponding author.
E-mail address: ifnata@ulm.ac.id (I.F. Nata).

https://doi.org/10.1016/j.jece.2020.104339
Received 9 June 2020; Received in revised form 21 July 2020; Accepted 27 July 2020
Available online 02 August 2020

solvothermal method produces nanoparticles that are stable, uniform particle size and good magnetification property [7,28].

Following our previous work [28], we have developed RH fiber and functionalized MNPs as biocomposites material. Amine group was introduced onto biocomposites structure by one-step reaction. Batch adsorption study was carried out to investigated adsorption behaviors of Mn(II) ion and total suspended solid by biocomposites magnetic nanoparticle rice husk cellulose based as adsorbent [17]. Moreover, concern on improving for high quality of functional material, we develop a biocomposites using waste material and modified surface which having chemical, physical and adsorption properties. In this study, we reported one-step synthesis to enhance amine functionalize MNPs on RH cellulose and its capability to capture Pb(II) ion in aqueous solution. The RHB-MH was synthesized in solvothermal method by variation of amine source, analyzed and also characterized which have high amine content on biocomposites. The kinetic adsorption type, effect pH of solution, Pb(II) ion adsorption isotherm and reusability of adsorbent were also investigated.

2. Material and methods

2.1. Material

The rice husk (RH) was taken from rice mill at Mempawah, South Kalimantan. Anhydrous sodium acetate ($C_2H_3NaO_2$), iron(III) chloride hexahydrate ($FeCl_3.6H_2O$), ethylene glycol ($C_6H_6O_2$), 1,6-hexanediamine ($C_6H_{16}N_2$, HDMA), lead(II) nitrate ($Pb(NO_3)_2$), hydrochloric acid (HCl), and sodium hydroxide (NaOH) were purchased from ACROS. The analytical grade for all the chemicals were chosen and used without further purification.

2.2. Rice husk cellulose preparation

Untreated RH was washed with distilled (DI) water for two times, and then dried at 105 °C. Dried RH was blended, then continuous with 60 mesh sieves and through to delignification step. The 40 % of RH soaked in solution of 1% NaOH, heated at 80 °C while stirring rate at 150 rpm for 2 h. After reaction, the RH washed with DI water until filtrate became neutral. The obtained product was rice husk cellulose (RH-D) after dried at 90 °C for 24 h.

2.3. Synthesis of amine functionalized rice husk magnetic nanoparticle biocomposites

The biocomposites was produced by one-step solvothermal reaction base on previous works [28] with slight modification. Briefly, the mixture 24 mL of ethylene glycol, 0.8 g of iron(III) chloride hexahydrate, and 1.8 g of sodium acetate anhydride, heated at 80 °C under stirred then added 5 g of RH-D. In order to functionalized surface of magnetic nanoparticle of 5, 7 and 9 mL of 1,6-hexanediamine was added for each batch, and keep at 200 °C for 6 h in Teflon stainless steel autoclave. After reaction, the reactor cooling manually, then black biocomposites was taken from the mixture by employing external magnetic field and then rinsed with DI water and 40 % of ethanol for 3 times. The biocomposites produced by 5, 7, and 9 mL of 1,6-hexanediamine were called RHB-MH1, RHB-MH2, and RHB-MH3, respectively. Naked MH was produced same procedure above without addition of fiber. As a control, biocomposites without addition of 1,6-hexanediamine (RHB-M) was also produced. In other hand, the all obtained materials were kept in DI water for future use as adsorbent.

2.4. Adsorption of Pb(II) ion onto amine functionalized rice husk magnetic nanoparticle biocomposites

The highest concentration of amine group on biocomposites was chosen as the best adsorbent for adsorption of Pb(II) ion. The Pb(II) ion removal was carried out in batch experimental. A 200 mL of a certain concentration of Pb(II) ion in 300 mL bottle and adjusting to pH 5, 6, and 7 with 1 M HCl or 1 M NaOH. A weighed amount of RHB-M and RHB-MH was added into bottle. The mixture was placed in a shaker (Firstek Scientific) at room temperature for certain contact time: 15, 30, 60, 120, 180, and 240 min. After experiment, the solution was separated by external magnetic field and filtered by using 0.2 µm PVDF membranes. Finally, the filtrate was analyzed for Pb(II) ion concentration using inductively coupled plasma atomic emission spectrophotometer (ICP-AES JY2000 2, Horiba Jobin Yvon). The Pb(II) ion adsorbed was described from the difference between initial and final adsorbate concentration. The data was taken in duplicate and the average value. In order to investigate the performance of biocomposites for repeated uses, the Pb(II) ions-loaded RBH-M and RBH-MH were desorbed by shaking in 0.1 N HCl for 4 h. After washing with DI water, the regenerated RHB-M and RHB-MH were used as the adsorbent for the next cycle. The recycle usage of adsorbent was repeated for three times in duplicate sample.

2.5. Characterization

The surface morphology of magnetic nanoparticle rice husk cellulose based biocomposites was examined by Field-emission scanning electron microscopy (FE-SEM, JOEL JSM-6500 F). The X-ray diffraction (XRD) measurement was investigated on Rigaku D/MAX-B X-ray diffractometer by using Copper K-alpha (CuKζ) radiation. The machine worked at 40 kV and 100 mA for operating voltage and current, respectively. Brunauer-Emmet-Teller (BET) surface area was evaluated by nitrogen adsorption-desorption using a Quantachrome, Autosorb-1 instrument. The superconducting quantum interference device (SQUID, LakeShore 7307) magnetometer was used to study magnetic property. Fourier transform infrared spectrometry (FT-IR, Bio-rad, Digilab FTS-3500) was taken to identify the functional groups on sample. For degradation material was studied by thermal gravimetric analysis (TGA) analysis using a Perkin Elmer, Diamond TG/DTA at 30 °C–1000 °C in nitrogen atmosphere flow (10 °C/min). The degradation material content in sample was studied by mass degradation from TGA curves. The surface charges of all materials were determined by zeta potential analyzer (Zetasizer 2000, Malvern Instrument, Malvern, UK). Retro-titration method was used for calculating amine content on biocomposites [29]. 50 mg of sample was added in to 25 mL of 0.01 M HCl and then shaken for 2 h at room temperature. 10 mL of supernatant was titrated by 0.01 N NaOH after through filtration. The amine group concentration calculation using:

$$C_{NH_2} = \left[\frac{(C_{HCl} \cdot V_{HCl}) - (5\, C_{NaOH} \cdot V_{NaOH})}{m_{sample}} \right] \quad (1)$$

where C_{HCl} and C_{NaOH} are the concentration of HCl solution (mmol/L) and concentration of NaOH solution (mmol/L), respectively, V_{HCl} is the volume of HCl solution (L), V_{NaOH} is the volume of NaOH used in the titration of non-reacted acid's excess (L) and m_{sample} is the weight of sample (g).

3. Results and discussion

3.1. Characterization of amine functionalized rice husk magnetic nanoparticle biocomposites

Rice husk has complex structure consist of hemicelluloses and lignin. The cellulose from RH was obtained by delignification. The result of RH cellulose was give different in the term of color, morphology, structure, and functional groups. The original color of RH is brown after treatment turns become gray (Fig. 1. inset). Treatment by NaOH cause breaking lignocelluloses structure of RH. As shown in Fig.1 by FE-SEM observation, the surface morphology has shown irregular shape and

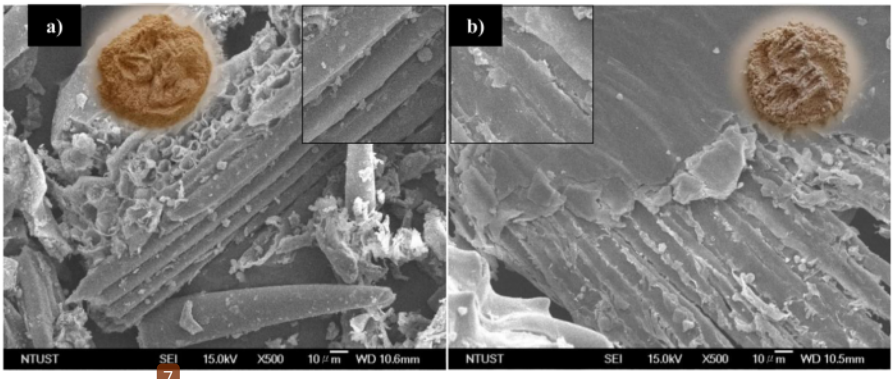

Fig. 1. FE-SEM images of (a) rice husk and (b) rice husk after delignification.

bumpy surface. After treatment, hemicelluloses, lignin and silica were removed from surface of RH [28,30]. It clearly showed the surface of RH smoother and extended in diameter.

Amine magnetic nanoparticle functionalization (MH) was successfully synthesized onto surface of rice husk cellulose. MH formation was generated in the presence of HMDA during the synthesis; different concentrations of HMDA have effects on the amount of amine concentration on MNPs. Amine source from HMDA as primary amine which contain of two hydrogen atoms and one atom nitrogen bonded on surface to form $-NH_2$. The schematic diagram of preparation magnetic nanoparticle rice husk cellulose based biocomposites as shown in Fig. 2.

The qualitatively technique using Ninhydrin which generated a Ruhemann's purple colored solution was used to identified amine group on the surface of biocomposite (Fig. 3, inset). Amine groups was confirmed which purple color developed for each biocomposites. The amine concentration on RHB-MH1, RHB-MH2 and RHB-MH3 were about 3.64; 12.3; 5.97 mmol/g, respectively. In addition, amine functionalization on RHB surface was also protected of iron for leaching to solution at low pH. In the case of aminated functinalization of magnetic nanoparticle coated on montmorillonite (Mt@MH), the amine content on RHB-MH almost same with Mt@MH [7]. Fig. 3 showed the surface texture of RHB in different concentration of HMDA and without addition of HMDA. It clearly revealed the round shaped of monodispersed magnetic nanoparticles were growth and covered surface layer of RH cellulose. HMDA is play role in the magnetic nanoparticles (Fe_3O_4) formation, when HMDA grafting on the core site of Fe_3O_4, it prevents to further growth and directly functionalized by amine group. Base on images, the Fe_3O_4 particle size of RHB-M (Fig. 3(a)) is 2-fold bigger than that all biocomposites which prepared by addition of HMDA. In other hand, the Fe_3O_4 was turn to aggregate for higher concentration of HMDA (Fig. 3(d)). Presumably, higher amount of amine group will block remaining ferric ion to growth become Fe_3O_4. The less amount of Fe_3O_4 on RHB-MH1 is shown in Fig. 3(b) compare Fe_3O_4 on RHB-MH2 (Fig. 3(c)). This observation also confirms by XRF result for Fe content on RHB-MH1, RHB-MH2 and RHB-MH3 are 90.12 %; 93.10 %; and 87.99 %, respectively.

The FT-IR spectra (Fig. 4) exhibited the resonance bands of amine group (1645 cm^{-1} and 1050 cm^{-1}), Fe—O (598 cm^{-1}), Si—O (1098 cm^{-1}) and OH (3400 cm^{-1}) bindings [7,28,30]. The RH and RHD founded Si—O band, it confirms that the RH content of Si. In addition, all samples for RHB spectra shown specific peak for Fe-O and amine group, it indicates the magnetic nanoparticle surface modification by one-step solvothermal treatment has been achieved. In the term of specific peaks for amine groups, RHB-MH2 has high peak intensity which related to concentration amine group on the surface of RHB. This result also confirm by Nynhidrin test and amine content for RHB-MH2.

The results obtained from the analysis of XRD are presented in Fig. 5. The typical spectrum of RH and RH-D could be observed for amorph and crystalline around peak at $2\theta = 16.2$ and 22.6, respectively. Delignification treatment was increased the crystalline index (CrI) of RH from 56.67% to 77.55%. The increasing number of CrI is due to releasing of silica, lignin and hemicelluloses. The amorph on lignocelluloses material is a less number of organized polysaccharide structure which the position is at low angle and broad peak [31]. Strong evidence crystalline of Fe_3O_4 was formed on surface of RH for specific peaks at 36°, 43°, 63° [32]. Again, high intensity of Fe_3O_4 peak for RHB-MH2 is elated with FE-SEM, FT-IR and XRF results.

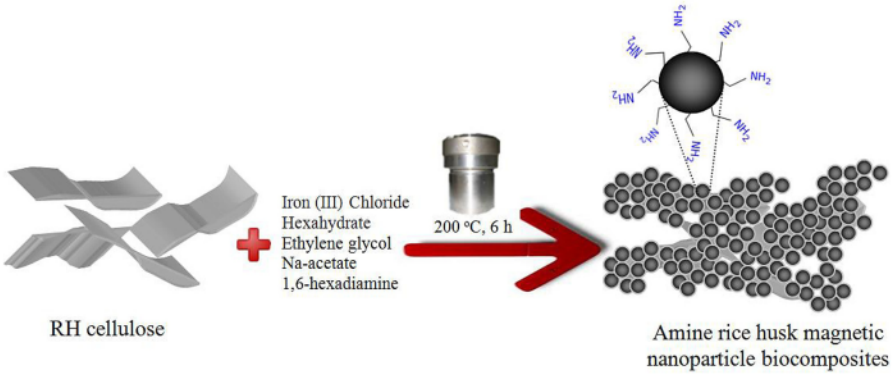

Fig. 2. Schematic preparation of amine rice husk magnetic nanoparticle biocomposites by solvothermal method.

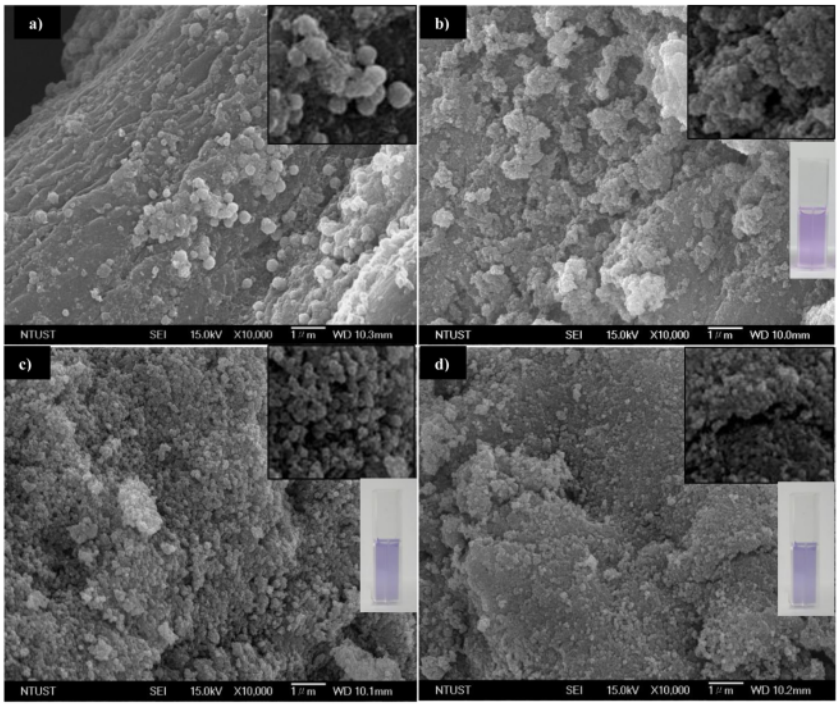

Fig. 3. FE-SEM images (a) RHB without addition of HMDA (RHB-M); (b) RHB with addition of 5 mL of HMDA (RHB-MH1); RHB with addition of 7 mL of HMDA (RHB-MH2); and (c) RHB with addition of 9 mL of HMDA (RHB-MH3).

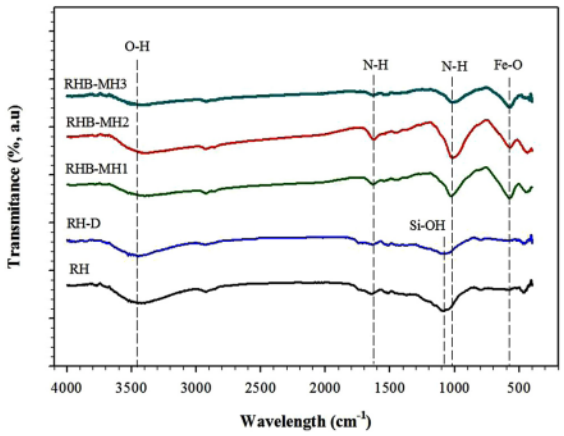

Fig. 4. IR spectra of rice husk (RH), rice husk cellulose (RH-D); rice husk biocomposites with addition of 5 mL of HMDA (RHB-MH1), rice husk biocomposites with addition of 7 mL of HMDA (RHB-MH2) and rice husk biocomposites with addition of 9 mL of HMDA (RHB-MH3).

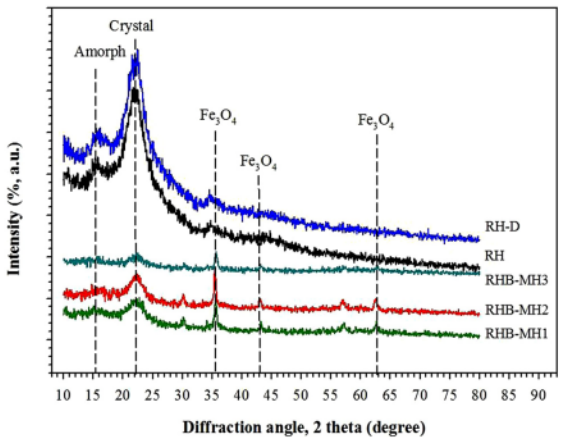

Fig. 5. Typical XRD pattern of rice husk (RH), rice husk cellulose (RH-D); rice husk biocomposites with addition of 5 mL of HMDA (RHB-MH1), rice husk biocomposites with addition of 7 mL of HMDA (RHB-MH2) and rice husk biocomposites with addition of 9 mL of HMDA (RHB-MH3).

Further analysis, RHB is a magnetite (Fe_3O_4) phase which has superparamagnetic properties, and will have reaction to external magnetic fie[6] which facilitate for separation. The biocomposites which contain of 0.5 g of fiber in 90 mL of water takes 50 s apart from the solution (Fig. 6 inset). The saturation magnetization measurement was investigated at room temperature employing SQUID analysis. Fig. 6 presents the result of ferromagnetic behavior of MH and RHB-MH2. The value of magnetic saturation of MH and RHB-MH2 are 67.94 and 16.47 emu/g, respectively. Decreasing magnetic saturation value of RHB-MH2 was 75.7 %, it is due to an appreciable amount of RH cellulose. It is apparent from Fig. 6 when MH in the composite form will loss amount of saturation value [33].

The nitrogen adsorption-desorption isotherm and distribution of pore diameter of RH-D and resulting biocomposites were shown in Fig. 7. The porosity is clearly difference from RH-D and biocomposites. The RH-D exhibits low up take nitrogen amount in isotherm, which confirm by low surface area of 1.309 m^2/g. In contrast, the all biocomposites show type II isotherm which higher adsorption nitrogen amounts as compare of RH-D [34]. The BET surface area (SBET) of RHB-MH2 is significantly increased 15-fold higher than RH-D. The

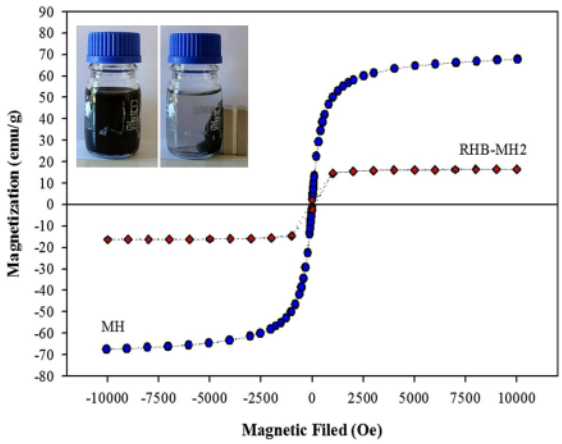

Fig. 6. Magnetization curve of magnetite (MH) and rice husk biocomposites with addition of 7 mL of HMDA (RHB-MH2) at room temperature.

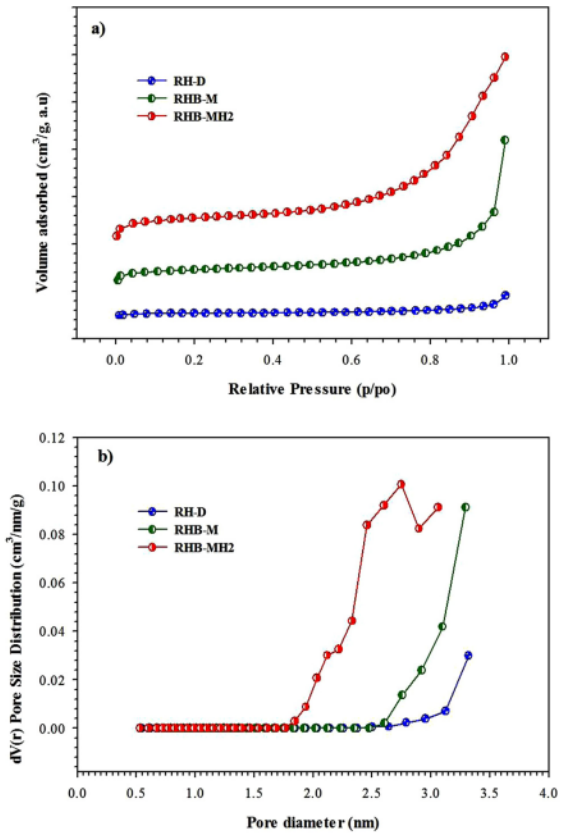

Fig. 7. The nitrogen adsorption-desorption (a) isotherm and (b) distribution of pore diameter of RH-D, RHB-M and RHB-MH2.

determinated SBET of RHB-M and RHB-MH2 were 9.113 m^2/g and 19.954 m^2/g, respectively. The pore volume (Fig. 7a) and pore diameter (Fig. 7b) analysis distribution of RH-D were smaller than those biocomposites. The formation of magnetic nanoparticle on surface of RH-D which leads to significant increased the surface area. The critical important for this results is technique to improved the surface area by

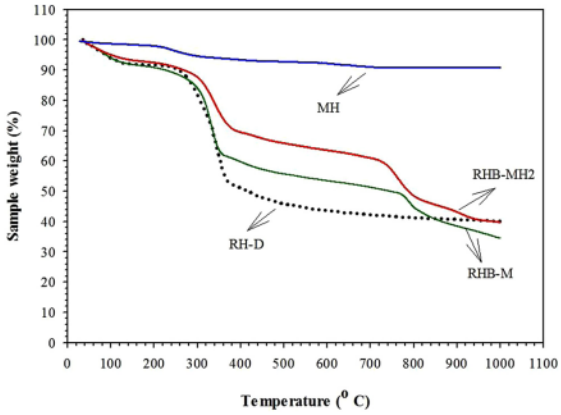

Fig. 8. TGA curve of rice husk (RH); rice husk biocomposites without of HMDA (RHB-M); rice husk biocomposites with addition of 7 mL of HMDA (RHB-MH2).

surface functionalization [35,36].

The gravimetric analysis was conducted for study typical degradation of biocomposites. Fig. 8 shows samples carbonized up to 1000 °C. In Fig. 8 for RH, there is a clear trend of decreasing weight for three stages. The 1st stage weight loss of RH located at temperature < 200 °C which dehydration or evaporation of light organic compound was occurred. The weight loss of 2nd stage was indicated at 200 °C–500 °C which degradation of hemicelluloses, cellulose and lignin and 3rd stage occurred at 700 °C [37]. For MH, it indicated only evaporation of water that proved by no significant weight loss during heating process. For RHB-M and RHB-MH2 also have 3 stages, the third stage is decomposition of amine groups on magnetite in the range 750 °C–800 °C. Interestingly, amine functionalized magnetic biocomposites produced the higher amount of magnetite. The excess amount base on TGA curve of RH, RHB-M and RHB-MH2 are 42.2 %; 50.98 %; 60.96 %, respectively. Based on this data, RHB-MH2 containing of magnetite 10 % higher than that RHB-M. This result also confirm by XRF and SEM observation.

3.2. Adsorption Kinetic of Pb(II) onto amine functionalized rice husk magnetic nanoparticle biocomposites

The rice husk biocomposites with amine functionalized magnetic nanoparticles was employed to adsorp Pb(II) ion. The RHB-MH2 was chosen as adsorbent with high amount of magnetic and amine groups. The experiment was conducted in batch process and investigated the optimum time for adsorption. The amount of Pb(II) ion being adsorbed by RHB-MH2 was considered difference of original concentration and concentarion after adsorption. As a control, the rice husk biocomposites without amine group also used as adsorbent for their capability to adsorb Pb(II) ion.

Pb(II) ion kinetic adsorption was evaluated with initial concentration of 50 mg/L at pH 5. The Pb(II) ion adsorbed capacity increases linearly up to 139 mg/g in 1 h adsorption as shown in Fig. 9. Afterward, the Pb(II) ion adsorbed rate increases slightly and constant to final of 163.9 mg/g was reached after 3 h. On this condition, a phase of equilibrium adsorption rate was occurred where there is no Pb(II) ion absorbed. Surprisingly, the optimum adsorption time is shorter than other type of adsorbent for same condition such as montmorillonite coated magnetic nanoparticle (Mt@MH) (MH@C) [7]. The data was fit to Pb (II) ion adsorption using 2 models, there are pseudo 1st order and pseudo 2nd order kinetic models. The calculation are described [38]:

$$\frac{dq_t}{dt} = k_1(q_e - q_t) \quad (1)$$

where q_e : Pb(II) ion adsorbed (mg/g) at equilibrium

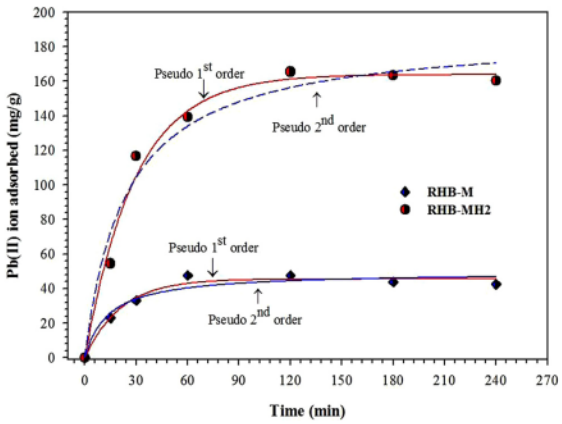

Fig. 9. Pb(II) adsorbed after adsorption at various of contact time onto RHB-M and RHB-MH2 at room temperature. Pb(II) initial concentration of 50 mg/L, pH 5, shaking rate 150 rpm.

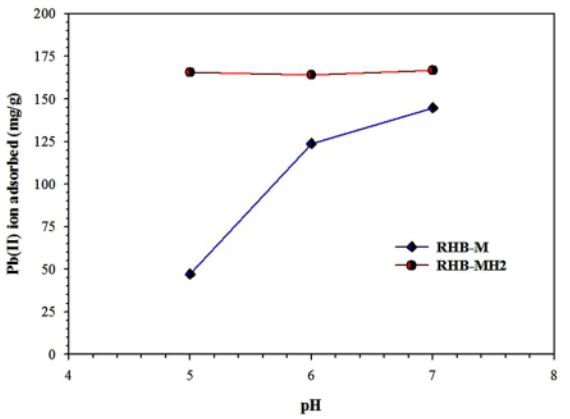

Fig. 10. Pb(II) adsorbed in various of pH onto RHB-M and RHB-MH2 as adsorbent. Pb(II) initial concentration of 50 mg/L, shaking rate 150 rpm, 2 h.

q_t : Pb(II) ion adsorbed (mg/g) time
k_1: is the rate constant of adsorption (min^{-1}).

$$\frac{dq_t}{dt} = k_2(q_e - q_t)^2 \quad (2)$$

where q_e : the maximum adsorption capacity (mg/g)
k_2: rate constant of the pseudo-2nd order equation (g/mg min)
q_t :the amount of Pb(II) adsorbed (mg/g).

The parameters these two kinetic models (equilibrium value of q_e and rate constant) were calculated by using non-linear regression and the result shown in Table 1. It seems that the pseudo 1st order kinetic model fitted well because of the higher number of coefficient correlation (r^2).

Based on adsorption maximum capacity of both adsorbent, the RHB-MH2 has better adsorption capacity 3.6-fold higher than RHB-M, this may occur because RHB-MH2 functionalized by amine group which has more ligand to capture ion. Beside, RHB-MH2 has a smaller diameter particle size, so it can provide high surface area, with high permeability and stable of mechanical and thermal properties.

3.3. The Effect of pH on Pb(II) ion adsorption onto amine functionalized rice husk magnetic nanoparticle biocomposites

It is known the equilibrium pH (pH_e) of solution is a key factor in the term of metal ion removal and also determine the main driving force for adsorption. Adsorption capacity of RHB-M and RHB-MH2 has influenced by pH of solution, this could be happened corresponds to protonation or deprotonation of adsorbent active side surface and also degree of ionization and species type [39,40]. In this research, only 5–7 range of pH were applied, because Pb(II) ion will precipitate on base condition to form Pb(OH)2. The ability of RHB-M and RHB-MH2 as adsorbents on Pb(II) ion adsorption can be seen in Fig. 10. It shows the optimum condition at pH 5 for RHB-M and RHB-MH2 adsorbent with adsorption capacity about 45.54 mg/g and 163.93 mg/g, respectively. For RBH-MH2, the trend of adsorption capacity is quite constant at pH 5, 6, and 7. In addition, capability of RHB-MH2 adsorption toward Pb (II) ion about 3.6-fold than that RHB-M at pH 5. The higher adsorption capacity of RHB-MH2 because presence amine groups on biocomposites surface, it makes surface stable in positive charged due to formation of–NH_3^+. Water solubility of amines is enhanced by hydrogen bonding involving these lone electron pairs, then interacted with Pb(II) ion as shown in Fig. 11. This phenomenon is also supported by surface charge measurement of materials (Fig. S1). The RHB-MH2 is positive charged at pH value < 7, then become negative charged at pH > 7. It proved that the formation of cationic amine groups on the range of pH 2−7. In addition, the surface charged of RH-D will shift to higher positive charged due to formation of magnetic nanoparticle.

The RBH-M have point zero charge (PZC) at pH about 5.5, so that the surface of RHB-M below PZC on positive charged and over PZC in negative charged. On this condition, the adsorption capacity of RHB-M will increased due to negative charged formation and electrostatic interaction is the dominant driving forces to capture Pb(II) ion. The protonation of Pb(II) ion in the range of pH facilitate electrostatic and complexation mechanism will have good capability for adsorption.

Table 1
The kinetic parameters of Pb(II) ion adsorption onto RHB-M and RHB-MH2 at room temperature.

Adsorbent	Kinetic Model	Parameter Constant	Value
RHB-M	pseudo 1st order	q_e (mg/g)	45.54
		k_1 (min)	0.048
		r^2	0.977
	pseudo 2nd order	q_e (mg/g)	49.50
		K_2 (g/mg min)	0.0015
		r^2	0.973
RHB-MH2	pseudo 1st order	q_e (mg/g)	163.93
		k_1 (min)	0.0342
		r^2	0.9875
	pseudo 2nd order	q_e (mg/g)	187.43
		k_2 (g/mg min)	0.0002
		r^2	0.972

3.4. Adsorption Isotherm of Pb(II) ion onto magnetic nanoparticle rice husk cellulose based biocomposites

The adsorption isotherm of Pb(II) ion toward RHB-M and RHB-MH2 was applied by using Langmuir adsorption model as shown in Eq. (3).

$$q_e = \frac{Q^o b C_e}{1 + bC_e} \quad (3)$$

Where:
q_e : amount of Pb(II) ion adsorbed at equilibrium (mg/g)
Q^o: maximal adsorption capacity (mg/g)
C_e: equilibrium concentration (mg/L)
b : adsorption constant (L/ mg).

Fig. 12 shows the adsorption isotherms of adsorbent, the isotherms could be well-fitted with Langmuir model as demonstrated by the square of correlation coefficients close to unity about 0.95 in Table 2.

The maximal adsorption capacity of RHB-M and RHB-MH2 were

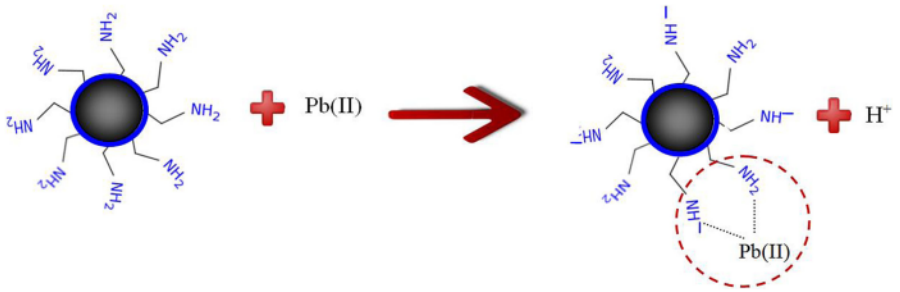

Fig. 11. Adsorption mechanism of Pb(II) ion on amine magnetic nanoparticle biocomposites.

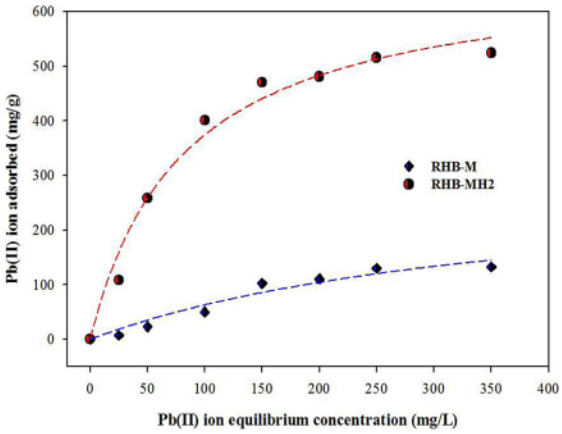

Fig. 12. Langmuir adsorption isotherm of Pb(II) ion onto RHB-M and RHB-MH2 as adsorbent at room temperature for 2 h, pH 5 and shaking rate 150 rpm.

Table 2
Parameter of Langmuir adsorption isotherm of Pb(II) ion onto RBH-M and RBH-MH2 at room temperature, 2 h, pH 5.

Isotherm constant	RHB-M	RHB-MH2
Q^o (mg/g)	300.78	680.19
b (L/mg)	0.0027	0.0123
r^2	0.952	0.982

Table 3
The maximum adsorption capacity of Pb(II) ion adsorption on different adsorbent.

Adsorbent	Adsorption capacity (mg/g)	pH_e	Reference
Magnetic-biochar	64.13	6	[5]
Magnetic polyethyleneimine	96.60	6	[4]
Fe_3O_4-SO_3H MNPs	108.93	7	[41]
Amine/thiol bifunctionalized MNPs	110.13	5	[6]
L-arginine modified magnetic chitosan	128.63	6	[9]
EDTA functionalized magnetic-biochar	129.31	6	[5]
Magnetic nanoparticle rice husk biocomposites (RHB-M)	300.78	5	This study
Amine functionalized rice husk magnetic nanoparticle biocomposites (RHB-MH2)	680.19	5	This study

300.78 mg/g and 680.19 mg/g, respectively. The adsorption capacity of RHB-M and RHB-MH2 for Pb(II) ion adsorption was also studied and reported by researcher using different adsorbents [4–6,9,41] as shown in Table 3. When compared to same Pb(II) ion adsorption, the adsorbed maximum capacity of RBH-MH2 approximately 5.26-fold higher than EDTA functionalized magnetic-biochar as highest adsorbent.

The prepared RHB-M and RHB-MH2 were successfully regenerated with nearly constant number of adsorption capacity. The recovered adsorbents were kept in 0.1 N HCl for 4 h with vigorous stirring to remove Pb(II) ion. The capacity of the recovered RHB-MH2 was slightly lower than that observed in the first run. For 4-repetition adsorption, only 4% uptake capacity decrease was observed (Fig. 13). In other words, the Pb(II) ion can be adsorbed on RHB-MH2 and the performance has not significantly deteriorated after several times repetition. The RHB-MH2 has been shown as a effective adsorbent for wastewater treatment, especially for metal ion removal in the wastewater effluent

4. Conclusions

Amine-rich functionalized on cellulose based magnetic nanoparticles rice husk biocomposites was successfully synthesized onto rice husk cellulose (RH). The rice husk cellulose was coated by aminated magnetic nanoparticle via one-step solvothermal method. The maximum adsorption capacity for Pb(II) ion was achieved up to 680.19 mg/g at pH_e ~ 5. The high up take capacity of RHB-MH2 is significantly increased due to amine functionalization on surface of magnetic nanoparticle. The electrostatic interaction was proposed as the primary driving force for Pb(II) ion adsorption. In addition, the RHB-MH2 has ferromagnetic properties which can facilitate the retrieval of adsorbent from waste stream by external magnetic field. The cellulose based magnetic nanoparticles rice husk biocomposites as promoting effective adsorbent for heavy metal ion removal from aqueous solution. The low cost raw material used also has good impact for waste utilization and

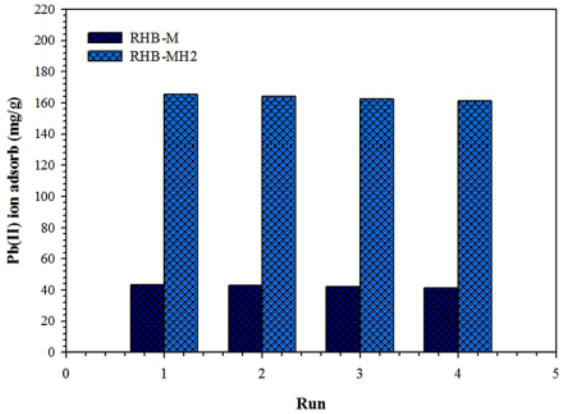

Fig. 13. Pb(II) ion adsorbed in number of recycle by RHB-M and RHB-MH2 as adsorbent at room temperature. Pb(II) initial concentration of 50 mg/L, pH 5, shaking rate 150 rpm for 2 h.

green environment.

Declaration of Competing Interest

The authors declare that they have no known competing financial interests or personal relationships that could have appeared to influence the work reported in this paper

Acknowledgement(s)

The authors acknowledge the financial support from Ministry of Research, Technology and Higher Education, Republic of Indonesia (contract No. 123.9/UN8.2/PP/2019).

Appendix A. Supplementary data

Supplementary material related to this article can be found, in the online version, at doi:https://doi.org/10.1016/j.jece.2020.104339.

References

[1] I. Martíne, A. Maria, P. Bernal, Environmental impact of metals, metalloids, and their toxicity, in: R. Deshmukh, D.K. Tripathi, G. Guerriero (Eds.), Metalloids in Plants, 2020, pp. 451–488.
[2] M.A. Eshlaghi, E. Kowsari, A. Ehsani, B. Akbari-Adergani, M. Hekmati, Functionalized graphene oxide GO-[imi-(CH2)2-NH2] as a high efficient material for electrochemical sensing of lead: synthesis surface and electrochemical characterization, J. Electroanal. Chem. 858 (2020) 113784.
[3] R. Naseem, S.S. Tahir, Removal of Pb(II) from aqueous/acidic solutions by using bentonite as an adsorbent, Water Res. 35 (2001) 3982–3986.
[4] X. Zhang, Y. Li, Y. Hou, Preparation of magnetic polyethylenimine lignin and its adsorption of Pb(II), Int. J. Biol. Macromol. 141 (2019) 1102–1110.
[5] M. Li, D. Wei, T. Liu, Y. Liu, L. Yan, Q. Wei, B. Du, W. Xu, EDTA functionalized magnetic biochar for Pb(II) removal: adsorption performance, mechanism and SVM model prediction, Sep. Purif. Technol. 227 (2019) 115696.
[6] J. Ji, G. Chen, J. Zhao, Preparation and characterization of amino/thiol bifunctionalized magnetic nanoadsorbent and its application in rapid removal of Pb (II) from aqueous system, J. Hazard. Mater. 368 (2019) 255–263.
[7] C. Irawan, I.F. Nata, C.-K. Lee, Removal of Pb(II) and As(V) using magnetic nanoparticles coated montmorillonite via one-pot solvothermal reaction as adsorbent, J. Environ. Chem. Eng. 1 (2019).
[8] R.R. Pawar, Lalhmunsiama, M. Kim, J.-G. Kim, S.-M. Hong, S.Y. Sawant, S.M. Lee, Efficient removal of hazardous lead, cadmium, and arsenic from aqueous environment by iron oxide modified clay-activated carbon composite beads, Appl. Clay Sci. 162 (2018) 339–350.
[9] S. Guo, P. Jiao, Z. Dan, N. Duan, J. Zhang, G. Chen, W. Gao, Synthesis of magnetic bioadsorbent for adsorption of Zn(II), Cd(II) and Pb(II) ions from aqueous solution, Chem. Eng. Res. Des. 126 (2017) 217–231.
[10] Y. Yang, Z. Zheng, M. Yang, J. Chen, C. Li, C. Zhang, X. Zhang, In-situ fabrication of a spherical-shaped Zn-Al hydrotalcite with BiOCl and study on its enhanced photocatalytic mechanism for perfluorooctanoic acid removal performed with a response surface methodology, J. Hazard. Mater. 399 (2020) 123070.
[11] Y. Wang, L. Yu, R. Wang, Y. Wang, X. Zhang, A novel cellulose hydrogel coating with nanoscale Fe0 for Cr(VI) adsorption and reduction, Sci. Total Environ. 726 (2020) 138625.
[12] J. Chen, X. Zhang, F. Bi, X. Zhang, Y. Yang, Y. Wang, A facile synthesis for uniform tablet-like TiO2/C derived from Materials of Institut Lavoisier-125(Ti) (MIL-125(Ti)) and their enhanced visible light-driven photodegradation of tetracycline, J. Colloid Interface Sci. 571 (2020) 275–284.
[13] A. Izadi, A. Mohebbi, M. Amiri, N. Izadi, Removal of iron ions from industrial copper raffinate and electrowinning electrolyte solutions by chemical precipitation and ion exchange, Miner. Eng. 113 (2017) 23–35.
[14] F. He, Z. Lu, M. Song, X. Liu, H. Tang, P. Huo, W. Fan, H. Dong, X. Wu, S. Han, Selective reduction of Cu2+ with simultaneous degradation of tetracycline by the dual channels ion imprinted POPD-CoFe2O4 heterojunction photocatalyst, Chem. Eng. J. 360 (2019) 750–761.
[15] F. He, Z. Lu, M. Song, X. Liu, H. Tang, P. Huo, W. Fan, H. Dong, X. Wu, G. Xing, Construction of ion imprinted layer modified ZnFe2O4 for selective Cr(VI) reduction with simultaneous organic pollutants degradation based on different reaction channels, Appl. Surf. Sci. 483 (2019) 453–462.
[16] A.H. El-Sheikh, F.S. Nofal, M.H. Shtaiwi, Adsorption and magnetic solid-phase extraction of cadmium and lead using magnetite modified with schiff bases, J. Environ. Chem. Eng. 7 (2019) 103229.
[17] E.Z. Effendi, Y.C. Hariady, M.D. Salaahuddin, C. Irawan, I.F. Nata, Utilization of rice husk cellulose as a magnetic nanoparticle biocomposite Fiber source for the absorption of manganese (Mn2+) ions in peat water, J. Kim. Sains Dan Apl. 22 (2019) 7 2019.
[18] I.F. Nata, A. Mirwan, D.R. Wicakso, C. Irawan, M.D. Isnaini, R. Fitriani, Adsorption of Fe^{3+} ion from aqueous solution onto rice husk biocomposite magnetic nanoparticle, IOP Conference Series: Earth and Environmental Science 506 (2020) 012006.
[19] V. Colapicchioni, S. Mosca, E. Guerriero, M. Cerasa, A. Khalid, M. Perilli, M. Rotatori, Environmental impact of co-combustion of polyethylene wastes in a rice husks fueled plant: evaluation of organic micropollutants and PM emissions, Sci. Total Environ. 716 (2020) 135354.
[20] I. Quispe, R. Navia, R. Kahhat, Life Cycle Assessment of rice husk as an energy source. A Peruvian case study, J. Clean. Prod. 209 (2019) 1235–1244.
[21] J.-H. Wu, C.-Y. He, Advances in cellulose-based sorbents for extraction of pollutants in environmental samples, Chromatographia 82 (2019) 1151–1169.
[22] M. Dominic, R. Joseph, P.M. Sabura Begum, B.P. Kanoth, J. Chandra, S. Thomas, Green tire technology: effect of rice husk derived nanocellulose (RHNC) in replacing carbon black (CB) in natural rubber (NR) compounding, Carbohydr. Polym. 230 (2020) 115620.
[23] S. Collazo-Bigliardi, R. Ortega-Toro, A. Chiralt, Improving properties of thermoplastic starch films by incorporating active extracts and cellulose fibres isolated from rice or coffee husk, Food Packag. Shelf Life 22 (2019) 100383.
[24] J. Tan, Z.-H. Deng, T. Wu, B. Tang, Propagation and interaction of magnetic solitons in a ferromagnetic thin film with the interfacial Dzyaloshinskii-Moriya interaction, J. Magn. Magn. Mater. 475 (2019) 445–452.
[25] Y. Zhao, M. Cao, J.F. McClelland, Z. Shao, M. Lu, A photoacoustic immunoassay for biomarker detection, Biosens. Bioelectron. 85 (2016) 261–266.
[26] Z. Lu, G. Zhou, M. Song, X. Liu, H. Tang, H. Dong, P. Huo, F. Yan, P. Du, G. Xing, Development of magnetic imprinted PEDOT/CdS heterojunction photocatalytic nanoreactors: 3-Dimensional specific recognition for selectively photocatalyzing danofloxacin mesylate, Appl. Catal. B 268 (2020) 118433.
[27] Z. Lu, G. Zhou, M. Song, D. Wang, P. Huo, W. Fan, H. Dong, H. Tang, F. Yan, G. Xing, Magnetic functional heterojunction reactors with 3D specific recognition for selective photocatalysis and synergistic photodegradation in binary antibiotic solutions, J. Mater. Chem. A 7 (2019) 13986–14000.
[28] I.F. Nata, M.D. Putra, D. Nurandini, C. Irawan, R. Fitriani, M.D. Isnaini, Rice husk fiber magnetic nanoparticle biocomposites: preparation and characterization, IOP Conference Series: Earth and Environmental Science 175 (2018) 1–6.
[29] B. Pi-Boleda, M. Bouzas, N. Gaztelumendi, O. Illa, C. Nogués, V. Branchadell, R. Pons, R.M. Ortuño, Chiral pH-sensitive cyclobutane β-amino acid-based cationic amphiphiles: possible candidates for use in gene therapy, J. Mol. Liq. 297 (2020) 111856.
[30] E. Menya, P.W. Olupot, H. Storz, M. Lubwama, Y. Kiros, M.J. John, Effect of alkaline pretreatment on the thermal behavior and chemical properties of rice husk varieties in relation to activated carbon production, J. Therm. Anal. Calorim. 139 (2020) 1681–1691.
[31] P. Kaur, P. Kaur, K. Kaur, Adsorptive removal of imazethapyr and imazamox from aqueous solution using modified rice husk, J. Clean. Prod. 244 (2020) 118699.
[32] H. Keshavarz, A. Khavandi, S. Alamolhoda, M.R. Naimi-Jamal, Magnetite mesoporous silica nanoparticles embedded in carboxybetaine methacrylate for application in hyperthermia and drug delivery, New J. Chem. 44 (2020) 8232–8240.
[33] X. Zhang, X. Kan, M. Wang, R. Rao, N. Qian, G. Zheng, Y. Ma, Mechanism of enhanced magnetization in CoFe2O4/La0.7Sr0.3MnO3 composites with different mass ratios, Ceram. Int. 46 (2020) 14847–14856.
[34] X. Li, Y. Xie, F. Jiang, B. Wang, Q. Hu, Y. Tang, T. Luo, T. Wu, Enhanced phosphate removal from aqueous solution using resourceable nano-CaO2/BC composite: behaviors and mechanisms, Sci. Total Environ. 709 (2020) 136123.
[35] X. Pi, F. Sun, J. Gao, Z. Qu, A. Wang, Z. Qie, L. Wang, H. Liu, A new insight into the SO2 adsorption behavior of oxidized carbon materials using model adsorbents and DFT calculations, J. Chem. Soc. Faraday Trans. 21 (2019) 9181–9188.
[36] F. Bi, X. Zhang, S. Xiang, Y. Wang, Effect of Pd loading on ZrO2 support resulting from pyrolysis of UiO-66: application to CO oxidation, J. Colloid Interface Sci. 573 (2020) 11–20.
[37] R. Xiao, W. Yang, X. Cong, K. Dong, J. Xu, D. Wang, X. Yang, Thermogravimetric analysis and reaction kinetics of lignocellulosic biomass pyrolysis, Energy 201 (2020) 117537.
[38] J. Qu, X. Tian, Z. Jiang, B. Cao, M.S. Akindolie, Q. Hu, C. Feng, Y. Feng, X. Meng, Y. Zhang, Multi-component adsorption of Pb(II), Cd(II) and Ni(II) onto microwave-functionalized cellulose: Kinetics, isotherms, thermodynamics, mechanisms and application for electroplating wastewater purification, J. Hazard. Mater. 387 (2020) 121718.
[39] V. Aghazadeh, S. Barakan, E. Bidari, Determination of surface protonation-deprotonation behavior, surface charge, and total surface site concentration for natural, pillared and porous nano bentonite heterostructure, J. Mol. Struct. 1204 (2020) 127570.
[40] S. Periyasamy, V. Gopalakannan, N. Viswanathan, Fabrication of magnetic particles imprinted cellulose based biocomposites for chromium(VI) removal, Carbohydr. Polym. 174 (2017) 352–359.
[41] K. Chen, J. He, Y. Li, X. Cai, K. Zhang, T. Liu, Y. Hu, D. Lin, L. Kong, J. Liu, Removal of cadmium and lead ions from water by sulfonated magnetic nanoparticle adsorbents, J. Colloid Interface Sci. 494 (2017) 307–316.

Selective adsorption of Pb(II) ion on amine-rich functionalized rice husk magnetic nanoparticle biocomposites in aqueous solution

ORIGINALITY REPORT

17%	17%	%	%
SIMILARITY INDEX	INTERNET SOURCES	PUBLICATIONS	STUDENT PAPERS

PRIMARY SOURCES

1	repo-dosen.ulm.ac.id Internet Source	7%
2	repositorium.sdum.uminho.pt Internet Source	2%
3	www.mdpi.com Internet Source	1%
4	cdmf.org.br Internet Source	1%
5	link.springer.com Internet Source	1%
6	www.tandfonline.com Internet Source	1%
7	pubs.rsc.org Internet Source	1%
8	www.researchsquare.com Internet Source	1%
	upcommons.upc.edu	

9	Internet Source	<1%
10	mafiadoc.com Internet Source	<1%
11	www.hindawi.com Internet Source	<1%
12	ejournal.undip.ac.id Internet Source	<1%
13	ppjp.ulm.ac.id Internet Source	<1%
14	en.wikipedia.org Internet Source	<1%
15	www.matec-conferences.org Internet Source	<1%
16	cwww.intechopen.com Internet Source	<1%
17	idoc.pub Internet Source	<1%
18	hdl.handle.net Internet Source	<1%
19	www.wydawnictwa.ipo.waw.pl Internet Source	<1%

Exclude quotes	Off	Exclude matches	Off
Exclude bibliography	On		